

Anterior cruciate ligament tibial insertion site is elliptical or triangular shaped in healthy young adults: high-resolution 3-T MRI analysis

Yasutaka Tashiro^{1,2}  · Gian Andrea Lucidi¹ · Tom Gale¹ · Kanto Nagai¹ · Elmar Herbst¹ · James J. Irrgang¹ · Yasuharu Nakashima² · William Anderst¹ · Freddie H. Fu¹

Received: 13 January 2017 / Accepted: 9 June 2017 / Published online: 24 June 2017
© European Society of Sports Traumatology, Knee Surgery, Arthroscopy (ESSKA) 2017

Abstract

Purpose To clarify the morphology of anterior cruciate ligament (ACL) tibial insertion site in healthy young knees using high-resolution 3-T MRI.

Methods Subjects were 50 ACL-reconstructed patients with a mean age of 21.4 ± 6.8 years. The contralateral healthy knees were scanned using high-resolution 3-T MRI. The tibial insertion sites of the anteromedial (AM) and posterolateral (PL) bundle fibres, and the ACL attachment on the anterior horn of lateral meniscus (AHLM) were segmented from the MR images, and 3D models were reconstructed to evaluate the morphology. The shape of ACL footprint was qualitatively analysed, and the size of AM and PL attachments and AHLM overlapped area was measured digitally.

Results Tibial AM and PL bundles were clearly identified in 42 of 50 knees (84.0%). Morphology of the whole ACL tibial insertion site was elliptical in 23 knees (54.8%) and triangular in 19 knees (45.2%), but not classified as C-shape in any knees. However, the AM bundle attachment was of C-shape in 29 knees (69.0%) and band-like in 13 knees (31.0%). Overlap of ACL on AHLM was found in 26 knees (61.9%), and the size of the overlapped area was $4.8 \pm 4.7\%$ of the whole ACL insertion site.

Conclusion 3D morphology of the intact ACL tibial insertion site analysed by high-resolution 3-T MRI was

elliptical or triangular in healthy young knees. However, the AM bundle insertion site was of C-shape or band-like. A small lateral portion of the ACL was overlapped with the AHLM. As for clinical relevance, these findings should be considered in order to reproduce the native ACL insertion site sufficiently.

Level of evidence III.

Keywords Anterior cruciate ligament · Morphology · Tibial insertion site · High-resolution · MRI · Young · Footprint

Abbreviations

ACL	Anterior cruciate ligament
AM	Anteromedial
PL	Posterolateral
MRI	Magnetic resonance imaging
ICC	Inter-class correlation coefficients
AHLM	Anterior horn of lateral meniscus

Introduction

Anatomical anterior cruciate ligament (ACL) reconstruction has been reported to be advantageous in restoring normal knee function and kinematics [1, 4, 14]. The principle of anatomical ACL reconstruction is to restore the dimension, collagen orientation and insertion site of the native ACL [6, 7]. Therefore, it is essential to understand the anatomy of the native ACL insertion site.

It has been well known that the anatomy of ACL has double-bundle of anteromedial (AM) and posterolateral (PL) fibres [2, 25, 35, 39]. Some studies have argued that ACL has a ribbon-like appearance of the mid-substance fibres and a “C”-shaped tibial insertion site [23, 30, 31].

✉ Freddie H. Fu
ffu@upmc.edu

¹ Department of Orthopaedic Surgery, University of Pittsburgh, 3471 Fifth Avenue, Pittsburgh, PA 15213, USA

² Department of Orthopaedic Surgery, Graduate School of Medical Sciences, Kyushu University, 3-1-1 Maidashi, Higashi-ku, Fukuoka 812-8582, Japan

Furthermore, recent cadaveric studies have reported substantial “direct fibres” ACL insertion on the more anterior part of its whole footprint [17, 19, 26], implying the importance of reproducing this localized area. However, most previous studies on ACL anatomy are based on older cadaveric specimens. Because degeneration of the ACL and significant decrease in mechanical properties can occur with the specimen age [38], the anatomical findings of older specimens might be different from younger ones. Focusing only on older specimens with degenerative changes in some part of ACL fibres may lead to an underestimation of ACL area in young individuals.

The geometry relation between the ACL tibial insertion site and the anterior horn of the lateral meniscus (AHLM) has also been focused on recently [3, 9, 10, 32]. It is important to understand the 3D relationship of the insertion site of these structures in order to avoid iatrogenic injuries to the AHLM during reaming of tibial bone tunnels [11]. Damage to the AHLM can cause deviation of the lateral meniscus and decrease of function as a secondary stabilizer of the knee [18, 28].

The purpose of this study was to clarify the morphology of ACL tibial insertion site in healthy young knees using high-resolution 3-T MRI. It was hypothesized that (1) intact ACL tibial insertion site would be of elliptical or triangular shape, (2) AM bundle attachment would be classified as C-shape, and (3) some ACL fibres overlap anterior horn of lateral meniscus. Findings from healthy young subjects would be relevant to the generation who needs ACL reconstruction.

Materials and methods

A total of 50 patients with a mean age of 21.4 ± 6.8 years old underwent bilateral 3-T MRI (Siemens Trio) during their time course after ACL reconstruction in a clinical trial [16]. The contralateral healthy knee data were used for this study. Thirty-three patients were male, and 17 were female. Physical examination showed no evidence of ACL dysfunction such as positive Lachman test or pivot-shift test. The MRI sequence used was three-dimensional double-echo steady state (3D DESS) with a high resolution of $0.365 \times 0.365 \times 0.70$ mm voxels (TR = 16.3 ms, TE = 4.7 ms, slice gap = 0 mm). The ACL tibial insertion was identified, and the attachment of anteromedial (AM) and posterolateral (PL) bundle fibres was distinguished from each other based on its appearance, principally using the sagittal MR images (Fig. 1a) and checked simultaneously with coronal and axial images using 3D processing software (Mimics®, Materialise, Leuven, Belgium). AM and PL bundle insertion sites were segmented on every image with a thickness of 4 pixels, and the 3D models

showing the morphology were created from the series of high-resolution 2D slices using the 3D reconstruction algorithm (Fig. 1b). In addition, the lateral meniscus was also segmented and the overlap of ACL fibres with the anterior horn of the lateral meniscus (AHLM) was determined (Fig. 1c).

Evaluation

Patients with intra-ligamentous cyst ($n = 2$), poor MR images due to artefact ($n = 2$) and difficulty in clearly distinguishing AM and PL ($n = 4$) were eliminated from the analysis. The shape of whole ACL tibial insertion site was categorized into elliptical (type I), triangular (type II) and C-shape (type III), according to a classification system, as previously described [12]. The shape of AM bundle tibial insertion was also assessed in axial view and classified as C-shape or band-like. Secondly, the ACL tibial insertion site was projected onto the axial plane of the tibia plateau, and the size of the AM and PL footprint and the AHLM overlapped areas was measured digitally, according to a previously reported method (Fig. 2) [8]. Medial–lateral width and anterior–posterior length of the whole ACL tibial insertion site and AHLM overlapped area were also measured.

The institutional review board (IRB) for human subject research in University of Pittsburgh (3500 Fifth Avenue, Pittsburgh, PA 15213, USA) approved all aspects of this study (ID: PRO09020493), and informed consent was obtained for all patients before enrolment.

Statistical analysis

In order to examine the reliability of MRI analysis, segmentation of the ACL tibial footprint was repeated twice with an interval of 3 months in ten knees by one observer (Y.T.) and repeated twice in ten knees by two independent observers (G.A.L. and Y.T.). The intra-class and the inter-class correlation coefficients (ICCs) were calculated, respectively. For the reliability of footprint shape classification, it was independently categorized by the two observers in all knees and the kappa coefficient value was calculated for the category value [27]. Power analysis was performed from the data reported in a previous study [12] (51, 33 and 16% for each shape type, Cohen’s Kappa statistic = 0.73, significant level = 0.05 and power = 0.80) to indicate sample sizes of 35 could address the questions.

Results

Anteromedial (AM) and posterolateral (PL) bundles could be clearly identified in 42 of 50 knees (84.0%).

Fig. 1 **a** Anteromedial (AM: blue) and posterolateral (PL: red) bundle fibres of the ACL are distinguished from each other at the tibial side, and the attachment is segmented from the sagittal MR images. **b** A 3D model of proximal left tibia with AM and PL insertion sites was created from the MRI slices using the Mimics® software. Medial meniscus is shown in this figure. **c** The lateral meniscus (LM) is segmented and shown in 3D. The overlap of ACL fibres and anterior horn of lateral meniscus (AHLM) is also segmented and reconstructed in 3D (green area indicated with arrow)

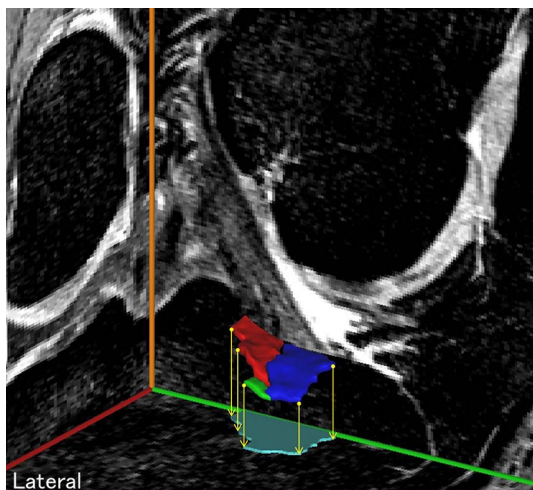
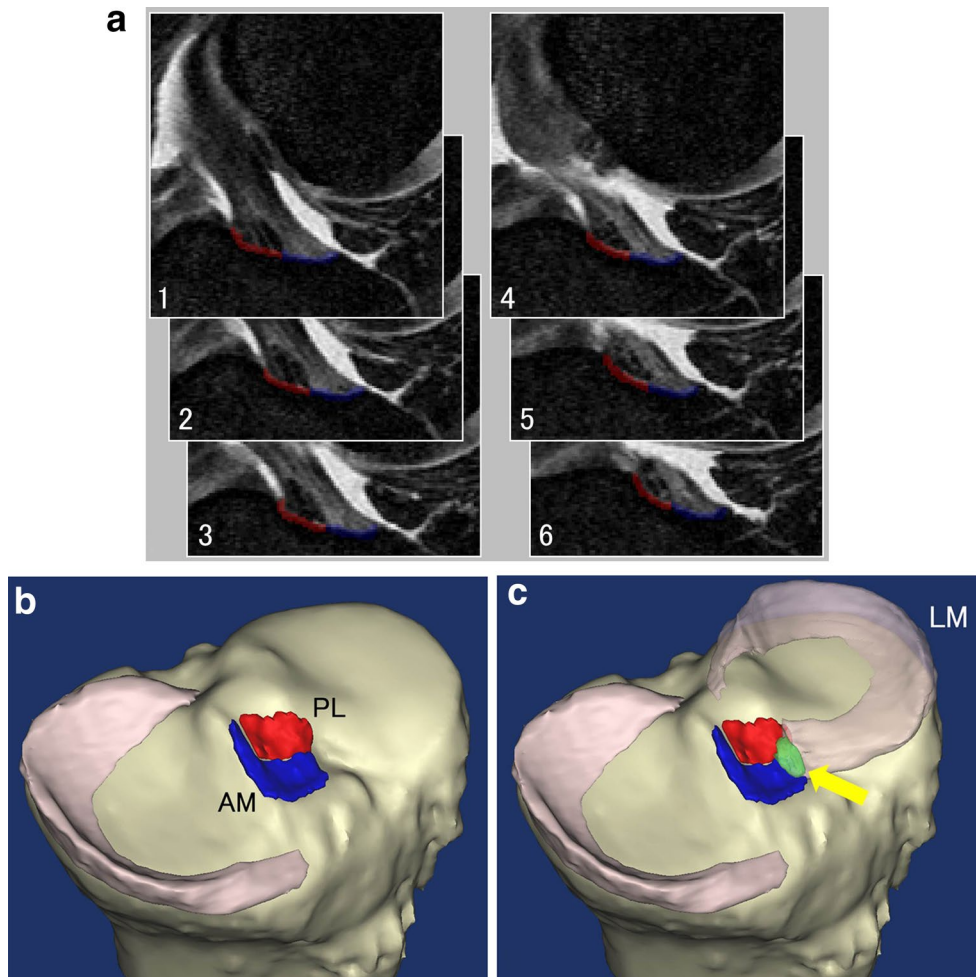


Fig. 2 For the measurement of footprint area (light blue), the ACL tibial insertion site was projected onto the axial plane which fits to tibia plateau. Each size of AM (blue), PL (red) footprint and AHLM overlapped (green) areas was measured digitally, according to a previously reported method [8]

Morphology of the whole ACL tibial insertion site was classified as elliptical (Fig. 3a) in 23 knees (54.8%), triangular (Fig. 3b) in 19 knees (45.2%) and C-shape in 0 knees (0.0%), whereas if PL bundle was eliminated and only AM bundle attachment was considered, it was of C-shape (Fig. 4a) in 29 knees (69.0%) and band-like (Fig. 4b) in 13 knees (31.0%). Overlap of ACL and anterior horn of LM (AHLM) was seen in 26 knees (61.9%), but no overlap was seen or just adjacent laterally in 16 knees (38.1%).

The whole ACL area of the ACL tibial insertion site was $182.7 \pm 41.1 \text{ mm}^2$ (Table 1). The AM bundle accounted for $53.6 \pm 12.5\%$, the PL bundle for $41.6 \pm 13.4\%$, and the LM overlapped area for $4.8 \pm 4.7\%$ of the whole ACL insertion site. Width of the whole ACL tibial insertion site was $14.5 \pm 2.2 \text{ mm}$, and length was $15.6 \pm 1.8 \text{ mm}$. Width of the LM overlapped area was $2.8 \pm 0.9 \text{ mm}$, and length was $4.8 \pm 1.7 \text{ mm}$.

The intra-observer reliability of MRI analysis was 0.93, 0.95, 0.94 and 0.90 in ICCs for the segmentation of whole ACL, AM and PL footprints, and overlap of ACL and

Fig. 3 Morphology of ACL tibial insertion site is shown in axial view. **a** An example of *elliptical* footprint of the whole ACL. **b** An example of *triangular* footprint. It was not classified as C-shape in any knee

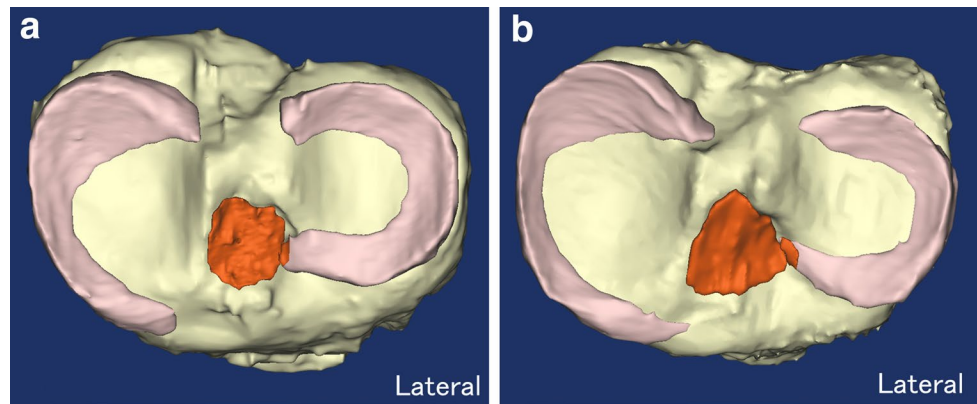


Fig. 4 If PL bundle was eliminated, AM bundle footprint looked C-shape (**a**) in 29 knees (69.0%) and band-like in 13 knees (31.0%) (**b**)

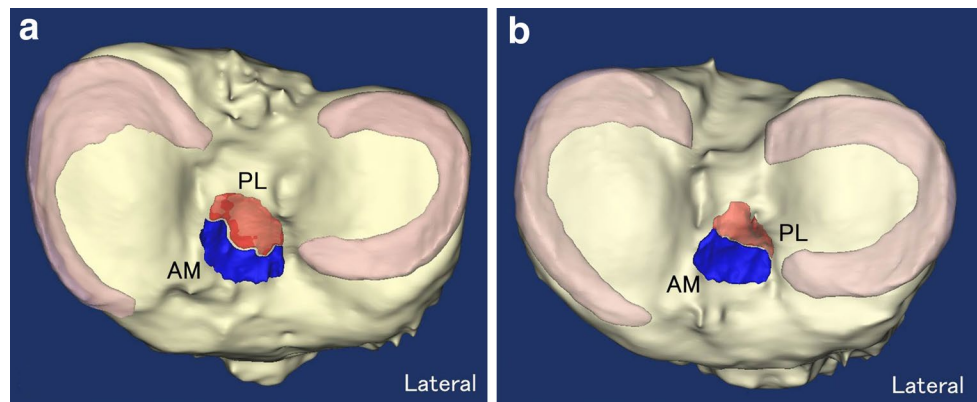


Table 1 Area of the ACL tibial insertion site

	Area (mm ²)	Percentage
AM bundle	98.0 ± 22.8	53.6 ± 12.5
PL bundle	76.0 ± 24.4	41.6 ± 13.4
LM attachment	8.7 ± 8.6	4.8 ± 4.7
Whole ACL	182.7 ± 41.1	100 ± 0.0

The values are presented as the mean ± standard deviation
AM anteromedial, PL posterolateral, LM lateral meniscus

AHLM, respectively. The inter-observer reliability was 0.87, 0.84, 0.89 and 0.89 in ICCs for whole ACL, AM and PL footprints, and overlap of ACL and AHLM. The reliability of classification for ACL tibial insertion site was 0.81.

Discussion

The most important finding of our study was that the ACL tibial insertion site in healthy young knees was attached to broad area with elliptical or triangular shape. A recent arthroscopic study classified the shape of ACL tibial insertion site in young subjects (mean 26 ± 11 years old) during

ACL reconstruction [12]. The rate of ellipse (51%) and triangle (33%) shape was similar to our study, but C-shape was seen in 16% in their study and this was different with our findings. While our MR images were obtained from healthy knees, tissue could be degenerated after ACL injury during the waiting period; thus, the degeneration in their subjects may have been affected by the period from the injury to surgery [20].

Functions and anatomy of double-bundle ACL fibres and elliptical (oval) or triangular shape of its tibial attachment have been reported by many previous studies [2, 13, 22, 24, 25, 35, 39], which was consistent with our study. A recent novel anatomical study on foetus knees has also reported ovoid tibial insertion of the ACL footprint and the presence of two well-distinguished bundles [5]. In contrast, it was reported by a recent cadaveric study that the ACL tibial insertion site was flat and of C-shape, and there were no central or PL inserting fibres in specimens with a mean age of 78 years [30]. This report is seemingly inconsistent with our findings of the whole ACL footprint; however, if the PL bundle was eliminated and only the AM bundle attachment was considered in our young MRI-based models, most of them were of C-shape or band-like, corresponding to the results of the previous cadaveric study. Area of the ACL tibial insertion site in the present study was similar to the

area in previous studies with middle-aged specimens [8], but it was somewhat larger than the area in other studies with older-aged specimens [13, 15, 29]. Because ageing can affect mechanical properties, vascularity, and cell proliferation of the ligament [21, 36, 38], higher age in specimens may affect degeneration of the ACL, especially for PL bundles that may resist rotatory loads [25].

ACL attachment on the anterior horn of lateral meniscus (AHLM) was found in over 60% of our cases. Even in those cases without attachment, ACL insertion on the tibia was found to be closely adjacent to the AHLM. Recent studies using histological analysis or scanning electron microscopy have also reported that a certain lateral portion of ACL tibial insertion overlaps the AHLM in human cadaveric knees [10, 32]. Damage to the AHLM can lead to extrusion of the lateral meniscus and decrease in knee stability after surgery [18, 28]. Surgeons should be careful to avoid damaging the AHLM when creating tibial tunnels.

The intact ACL in healthy young knees was analysed using high-resolution 3-T MRI, and it was considered as the novelty of our study. The use of high-resolution images and strong magnetic field made it possible to visualize anatomical structures precisely [33, 34, 37] and allowed to clearly differentiate AM and PL bundles insertion sites. Computational 3D reconstruction was useful in visualizing the morphology of ACL tibial insertion site, which was uneven and difficult to fully understand only with 2D images.

It is acknowledged that there are some limitations to our study. It was difficult to dissect healthy young knee specimens with intact ACL. Therefore, high-resolution 3-T MRI was used for the analysis and high inter-class reproducibility was shown. Secondly, the femoral side was not described in our study. It was not easy to differentiate AM and PL bundles for the femoral side with high accuracy in our MR images; therefore, only tibial side was analysed.

The finding of our study is of clinical relevance. This may be associated with the creation of tibial tunnels in ACL reconstruction. Considering the ACL tibial insertion site as an anteromedially localized area such as C-shape, based only on the knowledge of high-age cadavers, may lead to reproduction of tibial footprint in extremely localized area. Not only the C-shaped (or band-like) AM area, but also the PL area should be taken into account in order to help restore the anatomical ACL insertion site. In addition, it is important to avoid damaging the anterior horn of lateral meniscus.

Conclusion

3D morphology analysis using high-resolution 3-T MRI showed the intact ACL tibial insertion site was elliptical or triangular, but not of C-shape in healthy young knees. The

AM bundle had a C-shape or band-like attachment. A lateral part of ACL was overlapped with the anterior horn of the lateral meniscus (AHLM). It is necessary to consider both AM and PL bundles attachment areas, as well as preserving the AHLM to reproduce the native ACL insertion site sufficiently.

Compliance with ethical standards

Conflict of interest The authors declare that they have no conflict of interest.

Funding This study was supported by NIH/NIAMS Grant #R01 AR056630. Y.T. was supported by JSPS Fellowships for Research Abroad (H27-787), Grant of The Japanese Orthopaedic Society of Knee, Arthroscopy and Sports Medicine, 2016 and International Research Fund for Subsidy of Kyushu University School of Medicine Alumni.

Ethical approval The institutional review board (IRB) for human subject research in University of Pittsburgh (3500 Fifth Avenue, Pittsburgh, PA 15213, USA) approved all aspects of this study (ID: PRO09020493).

Informed consent Informed consent was obtained for all patients before enrolment.

References

1. Abebe ES, Utturkar GM, Taylor DC et al (2011) The effects of femoral graft placement on in vivo knee kinematics after anterior cruciate ligament reconstruction. *J Biomech* 44:924–929
2. Duthon VB, Barea C, Abrassart S, Fasel JH, Fritschy D, Menetrey J (2006) Anatomy of the anterior cruciate ligament. *Knee Surg Sports Traumatol Arthrosc* 14:204–213
3. Ellman MB, LaPrade CM, Smith SD et al (2014) Structural properties of the meniscal roots. *Am J Sports Med* 42:1881–1887
4. Fernandes TL, Fregni F, Weaver K, Pedrinelli A, Camanho GL, Hernandez AJ (2014) The influence of femoral tunnel position in single-bundle ACL reconstruction on functional outcomes and return to sports. *Knee Surg Sports Traumatol Arthrosc* 22:97–103
5. Ferretti M, Levicoff EA, Macpherson TA, Moreland MS, Cohen M, Fu FH (2007) The fetal anterior cruciate ligament: an anatomic and histologic study. *Arthroscopy* 23:278–283
6. Forsythe B, Kopf S, Wong AK et al (2010) The location of femoral and tibial tunnels in anatomic double-bundle anterior cruciate ligament reconstruction analyzed by three-dimensional computed tomography models. *J Bone Joint Surg Am* 92:1418–1426
7. Fu FH, van Eck CF, Tashman S, Irrgang JJ, Moreland MS (2015) Anatomic anterior cruciate ligament reconstruction: a changing paradigm. *Knee Surg Sports Traumatol Arthrosc* 23:640–648
8. Fujimaki Y, Thorhauer E, Sasaki Y, Smolinski P, Tashman S, Fu FH (2016) Quantitative in situ analysis of the anterior cruciate ligament: length, midsubstance cross-sectional area, and insertion site areas. *Am J Sports Med* 44:118–125
9. Fujishiro H, Tsukada S, Nakamura T, Nimura A, Mochizuki T, Akita K (2015) Attachment area of fibres from the horns of lateral meniscus: anatomic study with special reference to the

- positional relationship of anterior cruciate ligament. *Knee Surg Sports Traumatol Arthrosc*. doi:[10.1007/s00167-015-3813-3](https://doi.org/10.1007/s00167-015-3813-3)
10. Furumatsu T, Kodama Y, Maehara A et al (2016) The anterior cruciate ligament-lateral meniscus complex: a histological study. *Connect Tissue Res* 57:91–98
 11. Furumatsu T, Ozaki T (2016) Iatrogenic injury of the lateral meniscus anterior insertion following anterior cruciate ligament reconstruction: a case report. *J Orthop Sci*. doi:[10.1016/j.jos.2016.04.016](https://doi.org/10.1016/j.jos.2016.04.016)
 12. Guenther D, Irrarázaval S, Nishizawa Y et al (2015) Variation in the shape of the tibial insertion site of the anterior cruciate ligament: classification is required. *Knee Surg Sports Traumatol Arthrosc*. doi:[10.1007/s00167-015-3891-2](https://doi.org/10.1007/s00167-015-3891-2)
 13. Harner CD, Baek GH, Vogrin TM, Carlin GJ, Kashiwaguchi S, Woo SL (1999) Quantitative analysis of human cruciate ligament insertions. *Arthroscopy* 15:741–749
 14. Iliopoulos E, Galanis N, Zafeiridis A et al (2016) Anatomic single-bundle anterior cruciate ligament reconstruction improves walking economy: hamstrings tendon versus patellar tendon grafts. *Knee Surg Sports Traumatol Arthrosc*. doi:[10.1007/s00167-016-4229-4](https://doi.org/10.1007/s00167-016-4229-4)
 15. Iriuchishima T, Ryu K, Aizawa S, Fu FH (2015) Proportional evaluation of anterior cruciate ligament footprint size and knee bony morphology. *Knee Surg Sports Traumatol Arthrosc* 23:3157–3162
 16. Irrgang JJ, Tashman S, Moore C, Fu FH (2012) Challenge accepted: description of an ongoing NIH-funded randomized clinical trial to compare anatomic single-bundle versus anatomic double-bundle ACL reconstruction. *Arthroscopy* 28:745–747
 17. Kawaguchi Y, Kondo E, Takeda R, Akita K, Yasuda K, Amis AA (2015) The role of fibers in the femoral attachment of the anterior cruciate ligament in resisting tibial displacement. *Arthroscopy* 31:435–444
 18. Kodama Y, Furumatsu T, Miyazawa S et al (2016) Location of the tibial tunnel aperture affects extrusion of the lateral meniscus following reconstruction of the anterior cruciate ligament. *J Orthop Res*. doi:[10.1002/jor.23450](https://doi.org/10.1002/jor.23450)
 19. Moulton SG, Steineman BD, Haut Donahue TL, Fontbote CA, Cram TR, LaPrade RF (2016) Direct versus indirect ACL femoral attachment fibres and their implications on ACL graft placement. *Knee Surg Sports Traumatol Arthrosc* 25:165–171
 20. Nakamae A, Ochi M, Deie M et al (2010) Biomechanical function of anterior cruciate ligament remnants: how long do they contribute to knee stability after injury in patients with complete tears? *Arthroscopy* 26:1577–1585
 21. Nakano N, Matsumoto T, Takayama K et al (2015) Age-dependent healing potential of anterior cruciate ligament remnant-derived cells. *Am J Sports Med* 43:700–708
 22. Odensten M, Gillquist J (1985) Functional anatomy of the anterior cruciate ligament and a rationale for reconstruction. *J Bone Joint Surg Am* 67:257–262
 23. Oka S, Schuhmacher P, Brehmer A, Traut U, Kirsch J, Siebold R (2016) Histological analysis of the tibial anterior cruciate ligament insertion. *Knee Surg Sports Traumatol Arthrosc* 24:747–753
 24. Otsubo H, Shino K, Suzuki D et al (2012) The arrangement and the attachment areas of three ACL bundles. *Knee Surg Sports Traumatol Arthrosc* 20:127–134
 25. Petersen W, Zantop T (2007) Anatomy of the anterior cruciate ligament with regard to its two bundles. *Clin Orthop Relat Res* 454:35–47
 26. Sasaki N, Ishibashi Y, Tsuda E et al (2012) The femoral insertion of the anterior cruciate ligament: discrepancy between macroscopic and histological observations. *Arthroscopy* 28:1135–1146
 27. Shrout PE, Fleiss JL (1979) Intraclass correlations: uses in assessing rater reliability. *Psychol Bull* 86:420–428
 28. Shybut TB, Vega CE, Haddad J et al (2015) Effect of lateral meniscal root tear on the stability of the anterior cruciate ligament-deficient knee. *Am J Sports Med* 43:905–911
 29. Siebold R, Ellert T, Metz S, Metz J (2008) Tibial insertions of the anteromedial and posterolateral bundles of the anterior cruciate ligament: morphometry, arthroscopic landmarks, and orientation model for bone tunnel placement. *Arthroscopy* 24:154–161
 30. Siebold R, Schuhmacher P, Fernandez F et al (2015) Flat mid-substance of the anterior cruciate ligament with tibial “C”-shaped insertion site. *Knee Surg Sports Traumatol Arthrosc* 23:3136–3142
 31. Śmigielski R, Zdanowicz U, Drwiega M, Ciszek B, Ciszowska-Łysoń B, Siebold R (2015) Ribbon like appearance of the mid-substance fibres of the anterior cruciate ligament close to its femoral insertion site: a cadaveric study including 111 knees. *Knee Surg Sports Traumatol Arthrosc* 23:3143–3150
 32. Steineman BD, Moulton SG, Haut Donahue TL et al (2016) Overlap between anterior cruciate ligament and anterolateral meniscal root insertions: a scanning electron microscopy study. *Am J Sports Med* 45:362–368
 33. Swami VG, Cheng-Baron J, Hui C, Thompson RB, Jaremko JL (2015) Reliability of 3D localisation of ACL attachments on MRI: comparison using multi-planar 2D versus high-resolution 3D base sequences. *Knee Surg Sports Traumatol Arthrosc* 23:1206–1214
 34. Tanenbaum LN (2006) Clinical 3T MR imaging: mastering the challenges. *Magn Reson Imaging Clin N Am* 14:1–15
 35. Tsukada H, Ishibashi Y, Tsuda E, Fukuda A, Toh S (2008) Anatomical analysis of the anterior cruciate ligament femoral and tibial footprints. *J Orthop Sci* 13:122–129
 36. Uefuji A, Matsumoto T, Matsushita T et al (2014) Age-Related differences in anterior cruciate ligament remnant vascular-derived cells. *Am J Sports Med* 42:1478–1486
 37. von Borstel D, Wang M, Small K, Nozaki T, Yoshioka H (2017) High-resolution 3T MR imaging of the triangular fibrocartilage complex. *Magn Reson Med Sci* 16:3–15
 38. Woo SL, Hollis JM, Adams DJ, Lyon RM, Takai S (1991) Tensile properties of the human femur-anterior cruciate ligament-tibia complex. The effects of specimen age and orientation. *Am J Sports Med* 19:217–225
 39. Zantop T, Wellmann M, Fu FH, Petersen W (2008) Tunnel positioning of anteromedial and posterolateral bundles in anatomic anterior cruciate ligament reconstruction: anatomic and radiographic findings. *Am J Sports Med* 36:65–72